

# Inverting the Relationship of Fuel and Coolant

W. Van Snyder  
16 January 2022

## Abstract

In EBR-II, fuel was contained within fuel pins, and surrounded by coolant. That relationship could be inverted in a future LMFBR: Motile fuel, composed of fine metallic particles mixed with sodium for thermal bond, contained within a hexagonal unit cell penetrated by coolant tubes. A plenum above the fuel connected to an exhaust port would remove fission-product gases, especially the powerful neutron poison xenon, and maintain pressure within the unit cell in the range of the pressures in the coolant tubes or surrounding environment, thereby eliminating radial strain. Fuel/container mechanical interaction would be reduced or eliminated. Fuel volume fraction would be increased, which would improve neutron economy, increase breeding ratio, reduce initial fuel load fissile enrichment, and reduce reactivity swings during burnup. Passive safety implications of this proposal have not been assessed.

## 1 Introduction

In [7, pp. 308-309], Till and Chang remark “to maintain a hard spectrum, the fuel volume fraction needs to be maximized in the core lattice design... [H]igher fuel volume fraction design gives better neutron economy, resulting in lower fissile enrichment, a higher internal conversion ratio, and a reduced reactivity swing during burnup.”

In contemporary reactors, fuel is contained within pins and surrounded by coolant. Figure 1 illustrates a proposal to invert that relationship: Contain fuel within a hexagonal unit cell, with coolant tubes passing through fuel, and surrounded by coolant. Choose the  $2\tau$  spacing between unit cells such that the velocities of coolant flowing around the unit cell and through the coolant tubes, and therefore the pressures in those regions, are the same.

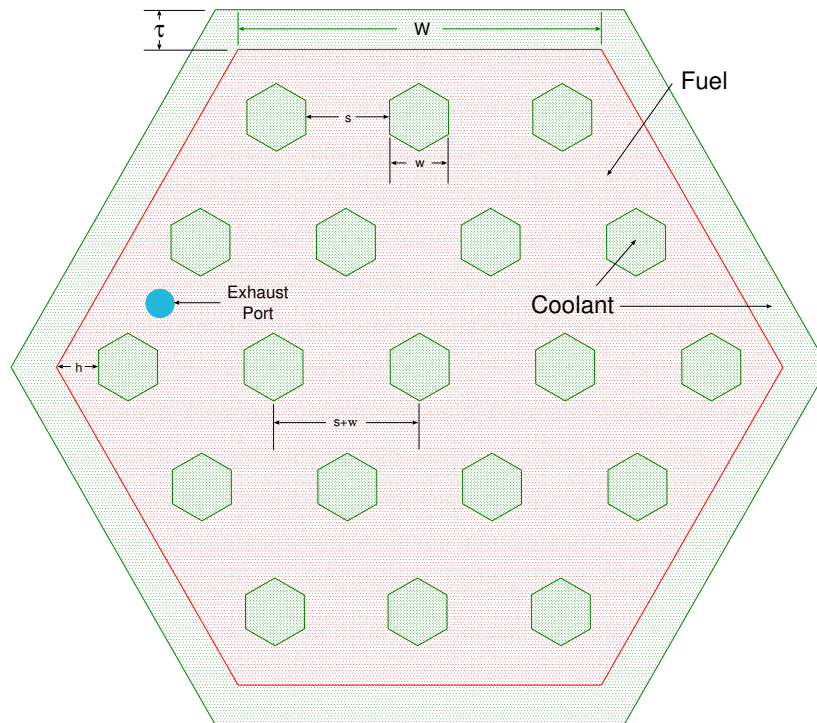


Figure 1: Unit cell,  $W = 3.241$  cm

Inverting the relationship allows a higher fuel volume fraction, with the attendant benefits described by Till and Chang. Unlike the case with numerous fuel pins within an assembly, it is feasible to connect an exhaust port to a plenum above the fuel, to remove fission-product gases, especially the powerful neutron poison xenon, and to maintain pressure within a unit cell in the range of the pressures in the coolant tubes or surrounding environment.

According to [7, p. 116], [3], and [6, p. 2], the primary limitation to fuel burnup in the Experimental Breeder Reactor II (EBR-II) was fuel pin cladding durability, and bundle-duct interaction due to radial fuel pin strain. Radial strain is eliminated by adjusting the pressure within the unit cell to be the same as the environment.

## 2 Fuel composition

One way to invert the relationship between fuel and coolant is to fabricate solid fuel slugs, somewhat smaller than a unit cell, with holes somewhat larger than coolant tubes. This might be possible by vacuum or injection casting. Drilling holes after casting would be undesirable. During burnup, fuel would expand, in bulk outward toward the edge of the unit cell, and inward toward coolant tubes. This might rupture the outer wall of the unit cell, or crush coolant tubes. To cope with that, lower initial fuel volume density, or more robust structure, would be necessary, both of which would decrease the fuel volume fraction.

To avoid those problems, fabricate fuel as small polydisperse particles mixed with sodium for thermal bond, as explained in [5]. This is only feasible in a sodium-cooled reactor. For a water-cooled reactor, it might be possible to use zinc for thermal bond, as explained in [5]. Bulk density of fuel would be in the range 65%-95%, depending upon particle size distribution, and the relationship of fuel particle sizes to container size and shape. As explained in [5], smaller average particle size reduces container boundary effects on fuel density, and increases fission product transfer to bond sodium.

With motile fuel, bulk expansion due to burnup would all be in the axial direction. With a plenum above fuel, to accommodate fuel expansion and fission-product gases, and with the plenum connected to an exhaust port, fuel would not put stress on the container, other than by its weight.

In EBR-II, fuel assemblies contained 91 pins [4, p. 2-2, 3-5]. Fabricating and filling a unit fuel cell should be simpler and less expensive than fabricating and assembling 91 fuel pins.

## 3 Structure

Construct a unit cell as a barrel with coolant tubes connected to the bottom. Fill it to an appropriate level with fuel, leaving a plenum above. Then connect a top to the coolant tubes and sides. Connect an exhaust port to the plenum, to remove fission-product gases and adjust pressure.

It is not practical to connect the plenums of a large number of small pins to an exhaust port. It is undesirable because those connections would interfere with coolant flow. Fission-product gas pressure is a significant contributor to radial strain and to cladding damage caused by fuel/container mechanical interaction (FCMI) [3, p. 96], and therefore a factor limiting burnup.

With fuel contained in a larger unit cell, penetrated by coolant tubes, it is easy to connect the plenum using a single exhaust port.

An exhaust port allows the pressure inside the fuel container to be adjusted. If internal and external pressure were the same, there would be no mechanical stress on the container, other than the weight of the fuel. There would be essentially no additional FCMI. The primary concerns in the design and materials of the container would be thermal-cycling stress, radiation damage, and fuel/container chemical interaction (FCCI). With FCMI and structure fraction reduced, a coating or other design changes to reduce FCCI should be feasible.

An exhaust port also allows to remove xenon, an important neutron poison, thereby increasing burnup and further improving the ability to maintain a hard neutron spectrum. Two exhaust ports per unit cell would

allow to flow argon, further removing xenon. Removing xenon during shutdown eliminates the “iodine pit” startup instability.

With internal pressure slightly less than external pressure, it should be possible to attach the coolant tubes, and the top and bottom of the assembly, by crimping instead of welding. It might be possible to construct the bottom and sides as a single piece by pressing, in the same way that beverage cans are made. Another alternative to welding is to thread the ends of the tubes, with opposite pitch direction, and to screw the tubes, top, and bottom together after filling, followed by crimping or welding the top and bottom to the side. Depending upon fuel mixture viscosity, it might be possible to prefabricate a sealed container, and fill it through later-sealed ports.

Because there is essentially no internal mechanical stress, and in particular no shear stress because fuel is motile, there is no need for internal structural members or wire wrap to maintain separation between coolant tubes. This decreases structure fraction and increases fuel fraction. If coolant tubes bow due to temperature gradients, a thin mid-level structure could be incorporated. This would have minimal effect on fuel volume fraction. Unlike the case with fuel pins surrounded by flowing coolant, it would not impede coolant flow or introduce turbulence.

Coolant tubes need not be circular. If they are hexagonal, arranged on a triangular lattice, the average distance from a fuel particle to the surface of a coolant tube is more uniform than with circular tubes. By choice of size and placement, spacing between edges of coolant tubes can be made uniform, thereby making the average distance between fuel particles and coolant more uniform throughout the unit cell, or intentionally nonuniform, to account for heating differences in different regions of the unit cell. For a particular cross-section area, a hexagonal tube has larger surface area than a circular one. This increases heat transfer from fuel to coolant, and increases structure fraction, for the same volume of coolant.

## 4 Design tradeoffs

For a single unit cell:

- Fuel volume fraction determines power density.
- Power density and temperature gradient along coolant tubes determine heat removal requirements.
- Coolant fraction, heat capacity, power density, and temperature gradient determine coolant flow velocity. These are related by the hydrodynamic heat balance equation [7, §14.4.2]

$$PALf_f = \rho ALf_c v C_p \Delta T \text{ or } v = \frac{f_f}{f_c} \frac{P}{\rho C_p \Delta T}, \quad (1)$$

where  $P$  is fuel power density ( $\text{kW}/\text{m}^3$ ),  $A$  is the cross-section area of the unit cell, including the surrounding coolant-flow region of thickness  $\tau$ ,  $L$  is the length of the reaction region of the unit cell (excluding the plenum and axial breeding blankets),  $f_f$  is fuel volume fraction,  $ALf_f$  is fuel volume,  $\rho$  is coolant density ( $\text{kg}/\text{m}^3$ ),  $f_c$  is coolant fraction,  $v$  is coolant flow velocity ( $\text{m}/\text{s}$ ),  $C_p$  is coolant heat capacity ( $\text{kJ}/\text{kg}/\text{K}$ ), and  $\Delta T$  is temperature gradient ( $\text{K}/\text{m}$ ) along the length  $L$  of coolant tubes.  $\rho A f_c v$  is coolant flow rate ( $\text{kg}/\text{s}$ ) and  $L\Delta T$  is total temperature increase.

- Horizontal temperature gradient within fuel determines number of and spacing between coolant tubes.
- Coolant flow velocity determines the pressure relationship between fuel and coolant.

Assume a hexagonal unit cell that contains hexagonal coolant tubes equally spaced on a triangular lattice. Assume that on the line from corner-to-corner of the unit cell, the edge-to-edge spacing of coolant tubes is  $s$ , and the spacing from the corner is  $h$  (see Figure 1). Then

$$(2n - 2)(s + w) + w + 2h = 2W, \text{ from which } w = \frac{W - (2n - 2)s - h}{2n - 1}. \quad (2)$$

Having coolant tube width  $w$ , unit cell edge width  $W$ , thickness  $t$  of coolant tube walls, and the number  $n$  of coolant tubes along one edge of the unit cell,  $f_c$ ,  $f_f$ , and the structure fraction  $f_s$  can be calculated.

The two-dimensional steady-state heat equation is a Poisson equation, *viz.*

$$\nabla^2 T = \frac{Q}{K_0}, \quad (3)$$

where  $T$  is temperature (K),  $Q$  is thermal power density (W/mm<sup>2</sup>), and  $K_0$  is thermal conductivity (W/mm/K). It was solved for a unit cell as shown in Figure 1. This is a proxy for a three-dimensional equation, assuming a 1-mm thick cross section of a unit cell with negligible temperature gradient and homogeneous Neumann boundary conditions, in the coolant flow direction. Within the cross section, the outer wall and coolant tube boundary conditions were Dirichlet conditions, with the coolant temperature taken to be 700 K. This is approximately the average temperature under EBR-II normal operating conditions [7, Fig. 7-4 p. 150], and is assumed to be representative of the mid plane of the reaction region.

Dimensions from EBR-II were used (Table 1). The edge-to-edge spacing  $s$  of coolant tubes was taken to be  $2R = 3.962$  mm, the same as the internal diameter of EBR-II fuel pins. The spacing  $h$  from the corner of the unit assembly was chosen to be  $1.45R$ , as a result of computational experiments, to make the maximum temperatures between coolant tubes, and between coolant tubes and the unit cell wall, approximately equal.

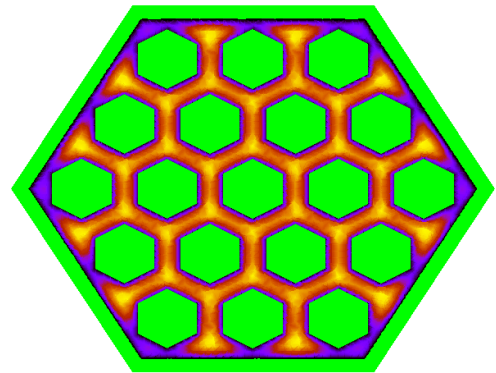
Table 1: EBR-II Assembly Dimensions [4, p. 3-5]

Assembly edge	$W$	33.58 mm
Fuel slug radius		1.829 mm
Fuel pin internal radius	$R$	1.981 mm
Cladding thickness	$t$	0.2286 mm
Fuel pins per assembly	$m$	91
Fuel fraction within one assembly	$f_f$	0.122
Power density of fuel	$P$	3.288 GW/m <sup>3</sup>
Assembly outer wall		1.016 mm
Temperature gradient	$\Delta T$	429.14 K/m

Table 2: Geometric and Thermal-Hydraulic Calculations

	$n = 3$	$n = 4$	$n = 5$	$n = 6$
$f_c$	0.5297	0.3571	0.2004	0.0782
$f_f$	0.3887	0.5480	0.6975	0.8214
$f_s$	0.0816	0.0949	0.1020	0.1004
$w$ mm	8.467	4.916	2.943	1.687
$\tau$ mm	1.293	0.7871	0.4059	0.1490
$(s + w)/w$	1.468	1.806	2.347	3.348
$v_2$ m/s	9.658	20.19	45.80	138.2
$\Delta p$ PSI	5.456	26.12	139.3	1282
$T_{\max}$ (K)	1030	1133	1238	1364
$T_{\text{avg}}$ (K)	828	909	988	1078
$\delta T_{\max}$ (K)	4.013	2.875	12.643	34.330

Figure 2: Temperatures



Calculations were undertaken with the number of coolant tubes  $n$  along each edge equal to 2, 3, 4, 5, and 6, i.e.,  $m = 3n(n - 1) + 1 = 7, 19, 37, 61,$  and 91 tubes total. Fuel power density was assumed to be the same as in EBR-II. For  $n = 2$  there were very hot spots at the edge of the unit cell, even though coolant tubes were in contact with the unit cell edge and  $h$  could not, therefore, be reduced. If  $s$  is increased

to  $3R$  and  $h$  is increased to  $2.03R$ , maximum temperatures in these zones were approximately equal, but exceeded fuel melting temperatures. For  $n > 3$ , coolant tube dimensions  $w$  were so small that fabrication would be difficult, and temperatures, pressure gradients, and coolant flow velocities were prohibitively large. These could be reduced by reducing  $s$  and increasing  $w$ , which would reduce  $f_f$ . For  $n > 4$ , the maximum temperature is greater than the boiling temperature (1156 K) of sodium. The results for  $n = 3, 4, 5$ , and  $6$  are shown in Table 2. Figure 2 shows the solution of the steady-state heat equation for  $n = 3$  (green regions are coolant-flow regions).

Volume fractions  $f_c$ ,  $f_f$ , and  $f_s$  include the unit cell external wall and the surrounding coolant-flow region of thickness  $\tau$ .

The coolant flow velocity  $v_2$  within coolant tubes was calculated from Equation (1) using  $\rho = 927 \text{ kg/m}^3$ ,  $C_p = 1.256 \text{ kJ/kg/K}$  [2, p. 14], and  $P$  and  $\Delta T$  the same as in EBR-II. The pressure change within coolant tubes was calculated using incompressible flow mass conservation, from which  $v_1 = f_c v_2$ , and Bernoulli's equation,  $\Delta p = \frac{\rho}{2} (v_2^2 - v_1^2) = \frac{\rho}{2} v_2^2 (1 - f_c^2)$ .  $\delta T_{\max}$  is the difference between the maximum temperatures in radial zones of thickness  $s + w$ . An iteration on  $h$  to reduce this would be simple, but would produce negligibly different overall results.

Calculations were repeated with several values of  $s$  in the range  $1.5R - 1.9R$ . Average and maximum temperatures have an approximately linear relationship to  $s$  in that range, with smaller values for smaller  $s$ .

Because the exhaust port is used to remove fission product gases, which have a very low flow rate, the exhaust port tube can be very small.

Because fission gas can be maintained at the same pressure as the environment, or slightly less, exhaust ports can be connected using fittings instead of welds.

Because fission product gases are removed, the plenum height can be less than in EBR-II fuel pins.

Rather than connecting each exhaust port externally using a long, thin, fragile tube, connect exhaust ports of adjacent unit cells using a U-shaped tube and self-closing ball-and-socket fittings, eventually leading to an external connection outside the core, or through a control-rod assembly. Unlike the case with numerous fuel pins within a fuel assembly, this would have minimal impact on coolant flow.

Incorporate axial breeding blankets into a longer unit cell, separated from the reaction region by a filter that allows sodium and fission gases to pass, but does not allow any but extremely small fuel particles to pass. To simplify spent-fuel processing, the filter could be made of sintered fuel, as explained in [5]. Absent vertical fuel convection, a filter would not be necessary.

## 5 Implications for post-irradiation fuel handling

As Koch explains in [4, p. 3-40], when a fuel assembly was removed from EBR-II for processing, it was necessary to cool it actively until it was disassembled. After disassembly, individual fuel pins were stored less densely, and natural atmospheric convection provided sufficient cooling. Storage for fuel pins awaiting processing was simple.

A unit cell as described here would need active cooling until it is opened and emptied for processing.

## 6 Implications for safety

In EBR-II, as temperature increased, fuel assemblies expanded, increasing separation between fuel pins, and the entire core structure expanded, increasing separation between fuel assemblies. This reduced neutron economy, providing a negative relationship of activity to temperature, and contributing to passive safety.

Fuel assembly structural elements in EBR-II were made of 304 (austenitic) stainless steel [1, p. 18]. Assume the unit cell is made of the same material. Relevant thermal expansion coefficients are shown in Table 3.

Table 3: Thermal expansion coefficients  $\mu\text{m}/\text{m}/\text{K}$ 

304 SS	18.7	Sodium	71
Uranium	13.9	Plutonium	46.7
Zirconium	5.7	U-19Pu-10Zr	19.2

With particulate fuel, when bond sodium and dissolved fission products expand due to increased temperature, they flow around fuel, which is 20.7 times more dense than sodium, increasing the height of sodium above fuel. Bond sodium and its dissolved fission products do not contribute to expansion of the bulk fuel mixture.

As burnup proceeds, uranium is converted to plutonium and actinides are converted to fission product metals having different thermal expansions, and fission product gases that largely escape from particulate fuel, as explained in [5]. Some fission product metals escape from fuel particles into bond sodium, and do not contribute to bulk fuel thermal expansion. The bulk fuel mixture thermal expansion coefficient, and its relationship to structural thermal expansion, depend upon the initial fuel alloy and the extent of burnup.

If fuel thermal expansion is less than for structure, as temperature increases, the ratio of active height to width decreases. If fuel thermal expansion is greater than for structure, as temperature increases, the ratio of active height to width increases. Which of these regimes holds in a particular reactor, or a particular unit cell, at a particular instant, depends upon the fuel alloy and the extent of burnup.

If structural elements that support fuel cells are similar to EBR-II, as temperature increases, separation between fuel cells would increase, similarly to fuel assembly separation in EBR-II.

Beyond these trivial observations, assessing the effect of thermal changes on passive safety is beyond the scope of this monograph. Whether a passively-safe reactor could be fueled using units described here is not known. Whether passive safety could be assured by incorporating structural elements that increase the space between unit cells as temperature increases is not known. Those are questions for people who have more knowledge and more tools than the author.

## References

- [1] T. Fei, A. Mohamed, and T. K. Kim. Neutronics benchmark specifications for EBR-II shutdown heat removal test SHRT-45R – Revision 1. Technical Report ANL-ARC-228 Rev. 1, Nuclear Engineering Division, Argonne National Laboratory, January 2013.
- [2] J. K. Fink and L. Leibowitz. Thermodynamic and transport properties of sodium liquid and vapor. Technical Report ANL/RE-95/2, Argonne National Laboratory, January 1995.
- [3] G. L. Hofman, L. C. Walters, and T. H. Bauer. Metallic fast reactor fuels. *Progress in Nuclear Energy*, 31(1/2):83–110, 1997.
- [4] Leonard J. Koch. *Experimental Breeder Reactor-II: An Integrated Experimental Fast Reactor Nuclear Power Station*. American Nuclear Society, 2008. ISBN 978-0-89448-042-1.
- [5] W. Van Snyder. Finely-divided metal as nuclear reactor fuel. *Nuclear Technology*, 208, March 2022.
- [6] Charles E. Till and Yoon Il Chang. Progress and status of the integral fast reactor (IFR) fuel cycle development. Technical Report ANL/CP-72650, Argonne National Laboratory, 1991.
- [7] Charles E. Till and Yoon Il Chang. *Plentiful Energy: The Story of the Integral Fast Reactor*. CreateSpace, 2011. ISBN 978-1466384606.